Laser backscattering image as non-destructive quality control technique for solid food matrixes: modelling fibre enrichment effects on physicochemical and sensory properties of cookies

Samuel Verdú*, José M. Barat, Raúl Grau.

Departamento de Tecnología de Alimentos. Universidad Politècnica de València, Spain

*Author for correspondence: Samuel Verdú

Address: Edificio 8E - Acceso F – Planta 0

Ciudad Politécnica de la Innovación

Universidad Politécnica de Valencia

Camino de Vera, s/n

46022 VALENCIA – SPAIN

E-mail: saveram@upvnet.upv.es

Abstract

This work was focused to model the effect of fibre enrichment on physicochemical and sensory properties of cookies by means of the image analysis of laser backscattering patterns. The study was done on four formulas, where besides the control, three fibre enrichment levels were included (5%, 10% and 20% w/w (d.b)). The impact on physicochemical and sensory properties of cookies was characterized based on the analyses of texture, thickness, area, mass increment, density, flux of solvents (water and milk), color, taste, mouth texture, etc. Moreover, the image analysis was carried out for collecting information from the interaction of a laser with two different matrices of cookie production chain: after mixing and forming phase (doughs) and after baking (end cookies). That information was obtained based on image descriptors generated from morphology of the observed laser patterns. Both studied matrixes offered different but complementary information, isolating the variance produced by the fibre enrichment in the case of doughs, while in the case of cookies the variance generated by heat treatment was also registered. The quantitative prediction of the physicochemical and sensory properties of cookies was improved when both information blocks were combined. The impact of fibre enrichment on cookies could be modelled using this imaging technique which could be the base to develop new non-destructive systems for on-line inspection during cookie processing which report physicochemical and sensory information in a rapid and non-destructive way.

Keywords: laser backscattering, imaging analysis, dough, cookie, fibre enrichment, modelling

1. Introduction

Improvement and optimization of both the most traditional and the most new processes in food industry had implicated developing more efficient control procedures to ensure the standards of quality and safety. This approach goes through reducing operation times, energy costs and waste products. Generally, substituting outdated devices, techniques, and modifying equipment materials are the main improvements in control and inspection modifications. In this sense, modifying and adapting new methods and techniques to the analysis and control procedures in productive processes could lead to major short-term improvements without high economic and time costs (Abdul Halim Lim, Antony, Garza-Reyes, & Arshed, 2015; Lim & Antony, 2016).

Thus, quickly collecting vast amounts of real time data from process chain operations is one of the most important tendencies of this approach using one or various techniques at the same time. This collected data is used as a database of entire production chain features, where information about all processes, operations and products could be combined to develop a map from which the knowledge about entire activity of production plant is increased because the possibility of using automatic learning applications, and to then improve decision making about any modifications required at any time.

The tendency in this research field is to create devices and techniques that operate no destructively (Chen, Zhang, Zhao, & Ouyang, 2013; Ropodi, Panagou, & Nychas, 2016). It implies the use of physicochemical principles for collecting data without coming into contact with the food products, in addition of avoid any modification of place, temperature, position, etc. In the food industry, those developments represent not only optimizing resources for processing, but also major advances in quality/safety control terms from raw material reception to end product storage because the reduction of plausible contamination points (Arendse, Fawole, Magwaza, & Opara, 2017).

Several techniques used to this purpose are light spectroscopy , ultrasounds, electronic tongues, image analyses, and some combination of them all (Barbin et al., 2015; Fuentes et al., 2017; Sendin, Manley, & Williams, 2017; Shi et al., 2018; Verdú et al., 2016; Wu et al., 2014; Xie, Chu, & He, 2017; Yang et al., 2018). Both the development and application of those techniques are conditioned by the physico-chemical nature of the selected food matrix, as well as the specific transformations that take place during a given operation. The structure and composition of matrix delimit the suitability of each technique to measure a given analyte and then condition the measurement system and environment. In this sense, the laser light backscattering image techniques fits with this approach since food matrix are frequently semi-transparent or opaque and allow the passage of light at specific wavelengths (Mireei, Mohtasebi, Massudi, Rafiee, & Arabanian, 2010). This technique has been successfully applied to fruit inspection, classification and drying, as well as moisture and solutes determination. Those applications have in common that have been applied in solid matrix to determine variables that imply important physic-morphological changes like phase changes, presence/absence of seeds, tissue damage, etc. Those results suggest that it could be very useful in processes where drying and changes of phase are the main transformations to obtain the products, as e.g in cereal derived products industry. These kinds of products are susceptible of being modified continuously because the introduction of new ingredients, which could produce modifications in the quality of end product and then need to be controlled. In the las years, one of the most modified properties has been the enrichment in fibre content with the aim of improving the healthy properties, although the physicochemical and sensory ones are usually committed. Some of the main cereal derived products within this tendency are cookies. A huge number of new cookies are commercialising each year with new fibres, which need to maintain their quality features to be accepted by consumers. The objective of this work is to study the influence of fibre enrichment on the physicochemical and sensory properties of cookies by means of imaging analysis of laser backscattering patterns with the aim of obtaining non-destructive information to develop quality predicting models.

2. Material and methods

2.1 Experiment procedure

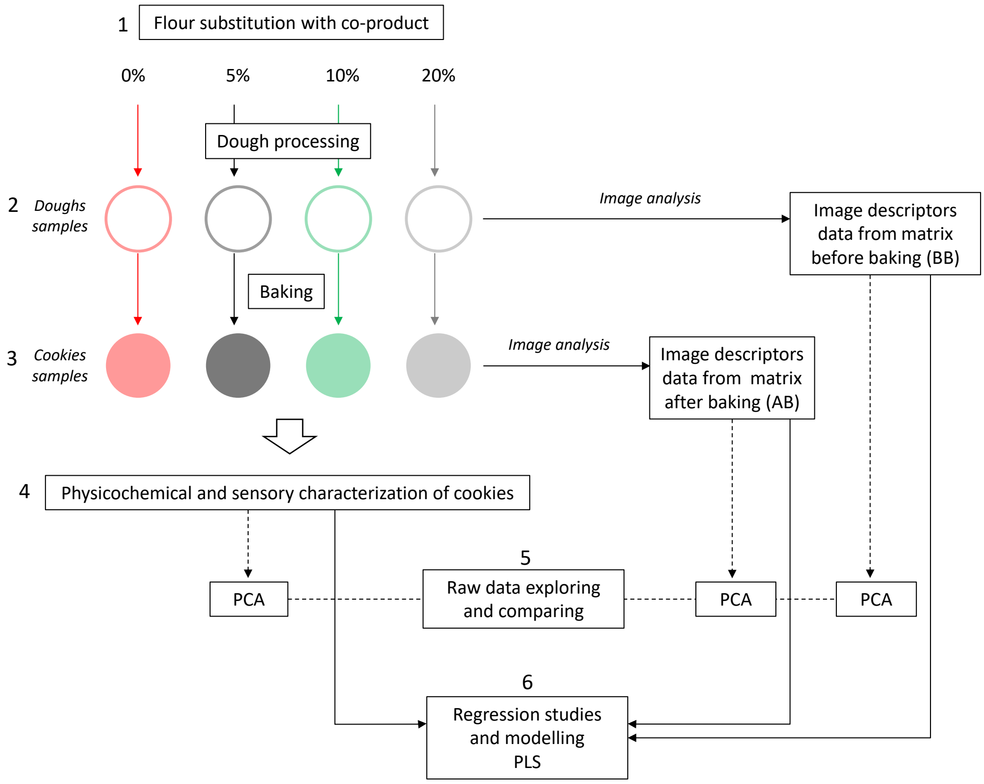

Figure 1. Scheme of experiment procedure. Numbers indicate the work phases.

The procedure of the experiment is schemed in Figure 1. The first phase was the preparation of flour mixes by substituting with the co-product in three different levels (5, 10 and 20% d.b), obtaining then four different mixes including the control (0%). The second phase was the processing of doughs. After forming the dough samples, images of laser backscattering patterns were captured and analyzed to extract image descriptors data from the food matrix before baking (*BB*). The third phase was the baking of formed doughs to obtain the cookies samples. Once cookies were produced, images of laser backscattering patterns were captured and analyzed to extract image descriptors data from the food matrix after baking (*AB*). The fourth phase was the physicochemical and sensory characterization of cookies to know the properties of each product. In the fifth phase, a comparative study was carried out between the characterization capability of the physicochemical/sensory data and the image data from both *BB* and *AB* matrix. The sixth and last phase was the study of the dependence between the physicochemical/sensory data and image data by means of regression studies.

2.2 Raw material

Cookies were produced by mixing wheat flour with the fibre source flour (tiger-nut milk co-product) flour at three substitution levels, 5%, 10% and 20% w/w, on a dry basis (d.b) of the wheat flour. These substitution levels were selected following Regulation (EC) No. 1924/2006 of the European Parliament and European Council. It indicates parameters for both "source of fibre foods" that require 3 g of fibre/100 g of product and "high fibre content foods" that require 6 g of fibre/100 g of product. Thus the 5% substituted formula was in accordance with the first denomination, the 10% substituted formula was in accordance with the second one, and the 20% substituted formula was included to evaluate the behaviour and feasibility of a larger amount of fibre in the process. The employed commercial refined wheat flour was obtained from a local producer (Molí del Picó-Harinas Segura S.L. Valencia, Spain), whose chemical composition was: 14.7±0.6% of proteins, 1.1±0.03% of fat, 14.5±0.5% of water, and 0.32±0.1 of ash (w.b). The alveographic parameters were also facilitated by the company, and were: P = 94±2 (maximum pressure (mm)), L = 128±5 (extensibility (mm)), W = 392±11 (strength (J^{-4})) and 0.73 of P/L.

The tiger-nut milk co-product was obtained from a local tiger-nut milk manufacturing plant, presented as wet fibrous flour. The co-product flour was dried to 14% of moisture (w.b) to be milled in a stainless steel grinder (Retsch GmbH, ZM 200, Haan, Germany) until around 271.1±8.1 µm, expressed as the average total volume size of the analysed flour particles (*D [4, 3]*). Finally, the proximate composition was 1.9±0.7% of proteins, 13.3±0.1% of fat, 14.1±0.4% of water, 1.86±0.1 of ash and 68.2±0.4% of the total dietary fibre (w.b). This proximate composition was analysed based on ICC (International Association for Cereal Science and Technology) standards 110/1, 156, 136, 105/2 and 104/1 for water, dietary fibre, fat, protein and ash, respectively. Sugar, baking powder (sodium bicarbonate, disodium diphosphate, rice flour and monocalcium phosphate,Royal, Kraft Foods Inc. Germany) and butter were obtained in a local commerce.

2.3 Cookies production

The cookies dough formula was wheat or fibre enriched flours (52%), sugar (17.4%), butter (14.5%), water (15.5%), baking powder (0.85%), salt (0.3%). Fat, sugar and water were mixed in a cooking robot (Thermomix®, Vorwerk, Germany) for 5 min at 75 rpm. After that, flour and baking powder was added and mixed for another 5 min at 200 rpm. The dough was kept at 4ºC for 24 h for better hydration of the fibre fraction. Then, cookies of X cm of diameter and 1 cm height were obtained using a metallic mould. The formed doughs were transferred to a baking tray and baked at 180ºC for 25 min in an oven (Mondial Forni, Verona, Italy). After baking, the samples were cooled at room temperature (20ºC) during 1 hour, and then packaged into plastic bags.

2.4 Physical properties

2.4.1 Texture analysis

Texture of samples were evaluated analyzing the maximum braking force (F_m). The texture analysis procedure was based on Islas-Rubio, de la Barca, Molina-Jacott, del Carmen Granados-Nevárez, & Vasquez-Lara (2014). The breaking force in g of the cookies was determined on texture analyzer TA-XT2 (Stable Microsystems, England) with a spherical-end accessory of 6.35 mm in diameter at the test speed of 1 mm/s. The hardness threshold was 1 g and the distance threshold was 1 mm. Twenty replies from each formula type were analysed. Individual samples of each formula were placed on the fracture accessory (code TA-101) and the ball penetrated the cookie until a complete fracture occurred.

2.4.2 Area, thickness and density

The area of cookies was measured by scanning them with a Canon Lide 120 scanner and using the ImageJ image analyser software. Thickness (*Th*) was measured five times on different places of each cookie using a Vernier caliper. Density (ρ) of cookies was calculated based on measured weight and volume (calculated from area and thickness).

2.4.3 Mass loss

All the samples rested for 30 minutes at room temperature after baking time and were weighed to determine mass loss during the process based on Equation 2:

$$\Delta M_B = \frac{m_f - m_0}{m_0} \cdot 100 \tag{1}$$

where ΔM is the mass increment in % , m_f is mass post-baking and m_o is the initial mass before baking

2.4.4 Diffusion of solvents

The diffusion of two model solvents, water and milk, was tested by mass uptake during the cookies immersion, following the experiment of Verdú et al., (2017). This assay was carried out by immersing full cookies, whose surface area and mass were known. Cookies were fixed by fine-tip tweezers to a universal support and were completely immersed in a glass with the solvent, which was placed on a precision balance (FV120, Anapesing, Spain). Mass uptake was recorded in 5-second intervals for 60 seconds. Diffusion was calculated as flux (J) using Equation 3:

$$J = \frac{g}{(A \cdot 2) \cdot s} \qquad (2)$$

where J is the flux of the solvent in the matrix in grams per cm^2 and second, g is the mass of the solvent updated at any time, A is the area of the cookie in cm^2, duplicated because of the two contact sides of the sample, and s is the time in seconds. Twenty replicates were used for each case. All the replicates were done under controlled room conditions of 20ºC/50% R.H.

2.5 Sensory properties

In order to test the effect of fibre enrichment of cookies, a sensory properties test was carried out. The study was done on the four formulas. The process was undertaken by 50 non-expert and untrained assessors, who are regular consumers of cookies and fibre enriched products. Tests were based on the semi-structured scales (AENOR, 2006) by which the attributes colour, odour, appearance, taste, mouth texture and global acceptance were assessed. These attributes were selected as the most descriptive for both industry and consumers of such products. A questionnaire was used, based on 10-cm lines where three reference points were represented (0 = unpleasant, 5 = acceptable, and 10 = pleasant) for each attribute. Each assessor evaluated four samples served at room temperature and coded them with a 3-digit random number. Samples were entire cookies.

2.6 Imaging system and descriptors

The system was based in capturing the generated pattern of laser backscattering onto dough and cookie surface because the light transmitting from bottom zone of sample. The capture system

(HD cam C615) was disposed into a dark cabin, to have an ambient away from light, at 15 cm vertically over sample surface, which was placed just in the middle of capture field. The laser pointer (650nm, 50mW, 3mm⌀) was perpendicularly disposed 20 cm under the samples, emitting to center zone of bottom surface. RGB images (3264×2448 pixels in the JPEG format) from 60 doughs and cookies (three lots of 20) from each fibre enrichment level were captured.

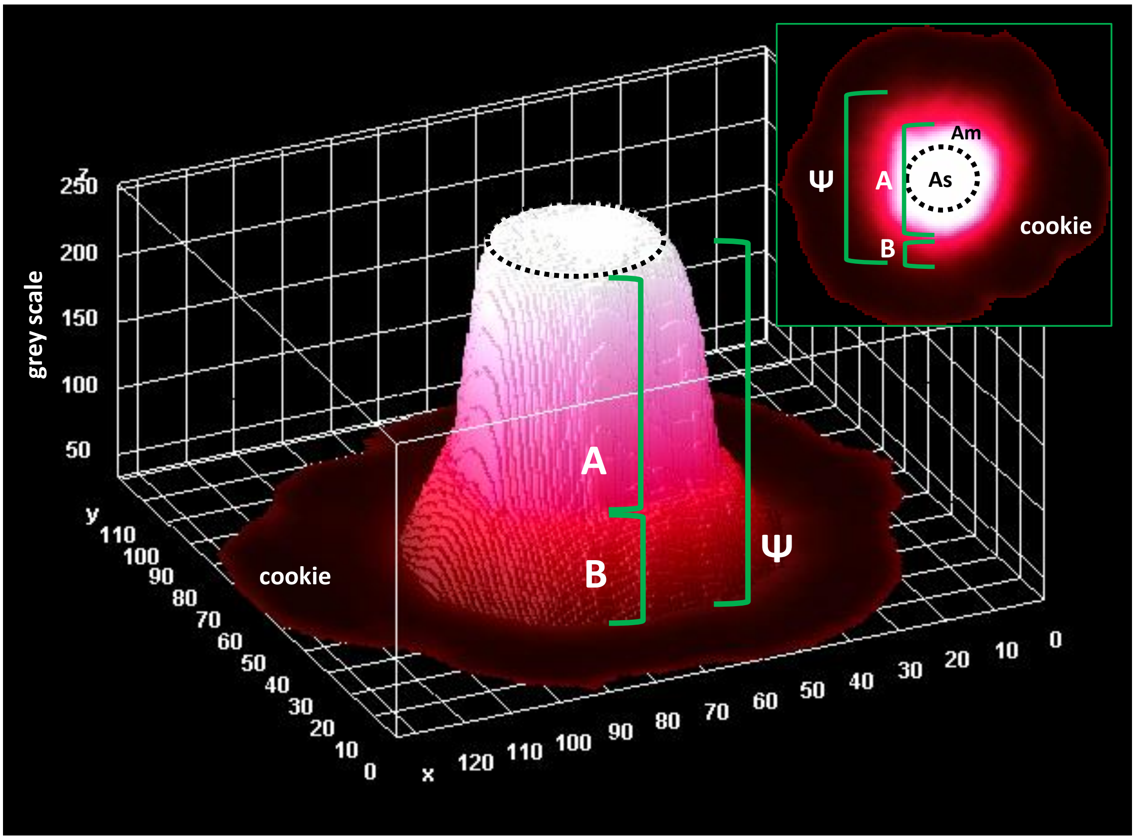

Figure 1. Laser-pattern morphology captured onto a cookie. Morphology and different zones of the direct descriptors: *Ψ*: complete light pattern; *A*: the lightest colour zone; *B*: the lowest colour saturated zone; *As*: saturated zone of *A*; *Am*: non-saturated zone of *A*.

The image descriptors were extracted after to the conversion of the RGB images to greyscale (8bits, 255 grey values), where different zones of lase-pattern morphology where delimited. Figure 1 shows an example of a captured laser-pattern. The images showed a typical diffraction pattern, where a maximum intensity peak is generated in the middle, commonly called Airy disk, and concentric rings which increase their size following the reduction of their intensity.

These rings are known as constructive and destructive interferences. This pattern followed the properties reported in other studies, where this technique is used to study different food matrix (Adebayo, Hashim, Abdan, & Hanafi, 2016; Mollazade et al., 2013; Verdú, Barat, & Grau, 2019). The developed image descriptors were delimited from this visual morphology. These descriptors were divided into two groups (direct and indirect), in function of their extraction procedure. The group of the direct descriptors represent absolute values of areas from laser-pattern colour zones. They are included in Figure 2 and were defined as following:

- Ψ: collects the area of pixels corresponding to entire light pattern (delimited within 45-255 of gray values)
- A: collects the area of pixels corresponding to the lightest colour zone of Ψ (delimited within 115-255 of gray values)
- B: collects the area of pixels corresponding to the darkest colour zone of Ψ (delimited within 45-114 of greys values)
- A_s *(A-saturated)*: collects the fraction pixels of A corresponding to saturated light (pixels with 255 of grey value)
- A_m *(A-minimum)*: collects the non-saturated area of A (delimited within 115-254 of grey values)

Equation 3 summarizes the direct descriptors system:

$$\Psi = A + B = (A_s + A_m) + B \qquad (3)$$

The optical interpretation of them would be the total transmitted light throughout the dough/cookie matrix for Ψ, the minimally altered transmitted light for A_s, while A_m and B represent indicators of scattered light amount.

The group of indirect descriptors represent the relationships between these five direct descriptors. They were generated by calculating all possible ratios among them. The ratios were A/Ψ; B/Ψ; A_s/Ψ; A_m/Ψ;B/A; A_s/A; A_m/A; B/A_s; A_s/A_m; B/A_m. Finally, image data was composed by a matrix of fifteen descriptors from each *BB* and *AB* matrix sample (5 direct and 10 indirect). All images were processed with the free software of image processing FIJI.

2.7 Statistical analyses

The physicochemical and image descriptors were explored and compared after applying multivariable statistical procedures with the aim of reducing the dimensionality of dataset. To this end, the multivariate unsupervised statistical method PCA (Principal Component Analysis) was used for comparing the variance collected by the physicochemical and sensory variables of cookies with which collected by image descriptors from doughs and cookies separately (Figure 1-phase 5). On the other hand, PLS-R (Partial Least Square Regression) was used to evaluate the dependence between the image descriptors from *BB* and *AB* matrix with the physicochemical and sensory properties of cookies (Figure 1-phase 6). This method was used to carry out linear regressions models between both data sets, which were evaluated based on R^2 of prediction, as well as root mean square errors (*RMSE*). The prediction models of physicochemical and sensory properties of cookies were done by using image data from all BB samples (240 samples), image data from all AB samples (240 samples), and both combined. Samples were divided into a training batch (60% of samples, 120 cookies) and a testing bacth (40% of samples, 80 cookies). Procedures were performed with PLS Toolbox, 6.3 (Eigenvector Research Inc., Wenatchee, Washington, USA), a toolbox extension in the Matlab 7.6 computational environment (The Mathworks, Natick, Massachusetts, USA). Physicochemical and sensory properties of cookies were studied by a one-way variance study (ANOVA). In those cases in which the effect was significant (P-value < 0.05), means were compared by Fisher's least significant difference (LSD) procedure.

3. Results and discussion

3.1 Physicochemical and sensory characterization of cookies

The effect of fibre enriching was significant on several properties of cookies. In despite of all formulas presented the same mass loss (*ΔM*, Table 1), assumed as water loss, the dimensions of cookies presented changes. The area suffered reductions of 5-7% (*ΔArea*) and thickness (*Th*) reach values with no differences. Both properties indicate retractions which had repercussion on increasing density (ρ) because the compaction of matrix of the product during heat treatment. However, texture was not modified (F_m). The compaction of matrix did not produce increase of resistance. This fact could be explained because although higher retractions were produced in matrix, the reduction of part of gluten and the disruption of a continue gluten-network produced a time a reduction of resistance. These retractions could be attributable because the tridimensional structure changes on co-product particles within dough matrix, which are produced when heat treatments are applied. These destructuring has been reported in several studies, where the reduction of particle size is proven in different dietetic fibre polymers when with different culinary heat treatments.

Table 1. Physicochemical and sensory data. Results of assays and regression studies.

Cookies descriptors	*CONTROL*	*5%*	*10%*	*20%*	*BB RMSEPred*	*AB RMSEPred*	*BB+AB RMSEPred*
Th (cm)	0,9±0,05a	0,94±0,02a	0,92±0,03a	0,88±0,04a			
F_m (N)	58,1±18,2a	55,2±12,3a	56,2±7,9a	61,1±5,4a			
*ΔArea (%)**	-20,1±1,8a	-26,36±2,3b	-27,53±2,4b	-25,11±2,5b	1,82	1,35	1,45
ΔM (%)	-21,7±0,8a	-20,9±0,8a	-21,5±1,0a	-21,8±0,9a			
*ρ (g/cm^2)**	0,6±0,01a	0,63±0,01b	0,69±0,01c	0,72±0,01d	0,01	0,00	0,00
*J_{W5}(g/m^2.s.10^{-4})**	5,1±0,18b	4,7±0,3b	4±0,8b	1,9±0,5a	0,53	0,58	0,59
*J_{W10}(g/m^2.s.10^{-4})**	3,3±0,06d	2,6±0,12c	0,2±0,4b	0,1±0,3a	0,22	0,40	0,29
*J_{M5}(g/m^2.s.10^{-4})**	3,1±0,4c	2,2±0,4b	1,8±0,6a	1,4±0,8a	0,25	0,18	0,16
*J_{M10}(g/m^2.s.10^{-4})**	1,9±0,2d	1,4±0,1c	1,1±0,2b	0,9±0,2a	0,16	0,12	0,13
Colour	5,1±1b	5,2±0,9b	5,1±0,5b	3,5±0,4a			
Odour	5,6±0,6a	5,6±0,8a	5,4±0,4a	5,4±0,3a			
Appearance	5,1±1b	5,1±1b	5,1±0,9b	3,7±0,2a			
*Taste **	6,8±0,6c	5±0,6b	4,9±0,7b	3,7±0,5a	0,35	0,33	0,38
Mouth texture	7±0,4a	6,7±0,2a	6,7±0,4a	6,6±0,6a			
*Global aceptability **	6,8±0,8c	5,2±0,9bc	4,9±0,5b	4,1±0,3a	0,17	0,20	0,20
*PC1(90.26%)**	8.1±1,2	0.99±0,9	-2.05±0.3	-7.1±0.2	2,04	1,70	1,94

Th: thickness; F_m: maximum braking force; *ΔArea*: area increment; *ΔM*: mass loss; ρ: density; J_w: water fluxes at 5 and 10 seconds; J_M: milk fluxes at 5 and 10 seconds; *PC1*: scores of the first principal component from the PCA of Figure 3A.

The consequence of those phenomena was the reduction of diffusion of used liquids because decrease of porosity. Both flux of water (*Jw*) and milk (*Jm*) were reduced with fibre enriching. Figure 2 shows the mean flux kinetics during the assay. Water presented higher diffusion than milk at any substitution level. However, the effect on milk was clearer for 5 % and 10%, which presented higher differences with control than water. Although the effect of natural dissolved solutes and dispersed particles into milk was evident, the effect of enrichment on matrix was common for both liquids. Data of fluxes from 5 and 10 minutes were taken as comparative base, because this interval of time presented the main differences and could adjust to a real time that consumer immerse the product before eat (Table 1). The observed effect match with other diffusional studies reported previously about fibre enrichment effect in wheat matrixes (Verdú et al., 2017), where increasing produce a drastic reduction of solvents diffusion, in that case water and sunflower oil.

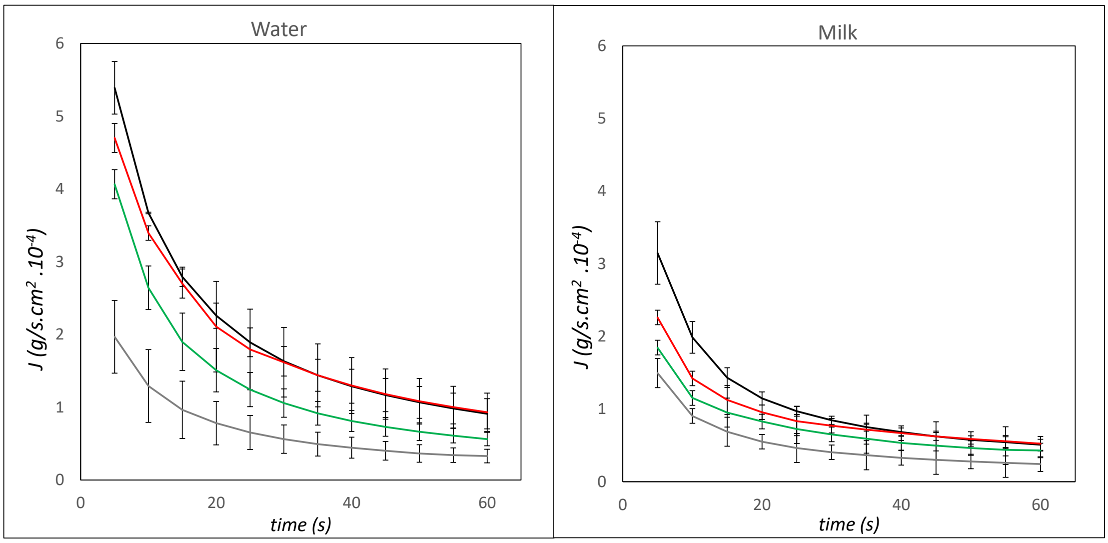

Figure 2. Diffusion of water and milk to cookies expressed in average of flux (*J*) g/s.cm^2. Black: control; Red: 5%; Green: 10%; Grey: 20%. Bars mark standard deviation of *J*.

The effect of enrichment affected only on some sensory properties. Colour, appearance, mouth texture and odour were the least affected. Colour and appearance presented significant reductions on scores at 20% of substitution, while odour and mouth texture were not modified.

In this sense, the result of non-affected mouth texture filled with the result observed previourly about resistance measured with texturometer (F_m). The most impact of enrichment was observed in taste and global acceptability, which should be mostly affected by taste modification. Then, the enrichment affected only on taste, however it is difficult to differentiate if this effect was produced by either only sensory attributes of the used fibre source or because the changes in taste dynamics during mastication due to the observed physical modifications.

To explore the weight of each affected variable on the global characterization of samples, PCA was performed. This procedure allowed knowing the relationship among variables and samples simultaneously. Figure 3-A shows the biplot generated from all physicochemical data, where the spontaneous clustering of samples and variables is represented. The ordering of samples (points represent the mean value of scores) followed the substitution level across PC1, from positive to negative section of this axis, which collected 90.26% of total variance. All variables presented high positive weigh with PC1, excepting density, which presented the inverse behaviour. This distribution allowed understanding the results above observed, which showed that the increase of density due to the retraction of matrix influenced the rest of variables in inversely proportional way.

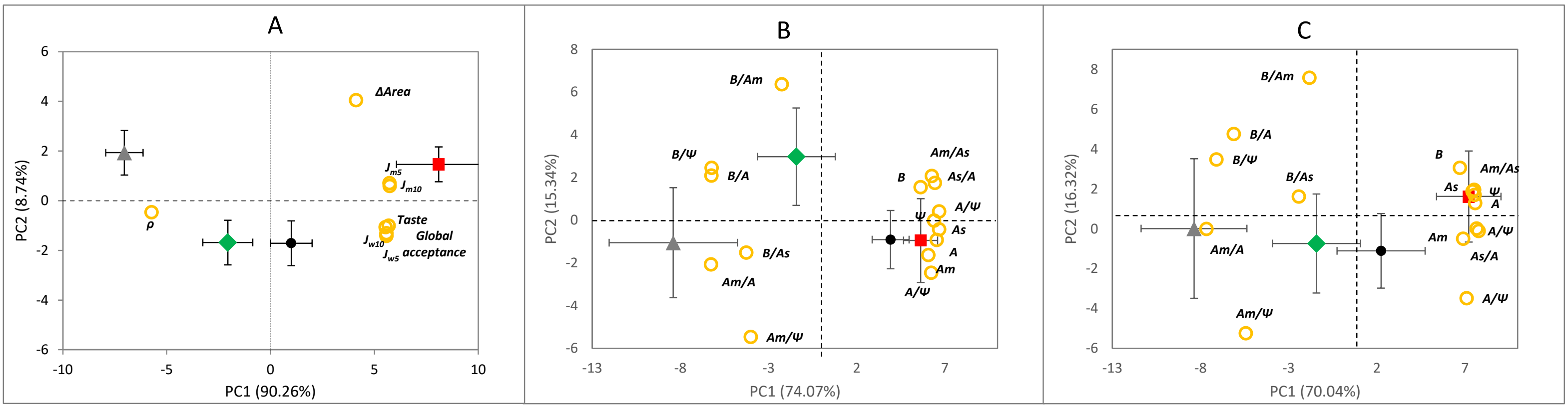

Figure 3. Biplots of PCA from physicochemical/ sensory data (A) and image descriptors data of matrix before baking (*BB*) (B) and matrix after baking (*AB*) (C). PCA scores are represented as

average and standard deviations (bars): Black: control; Red: 5%; Green: 10%; Grey: 20%; Yelow: variables.

3.2 Imaging descriptors data exploring and comparing

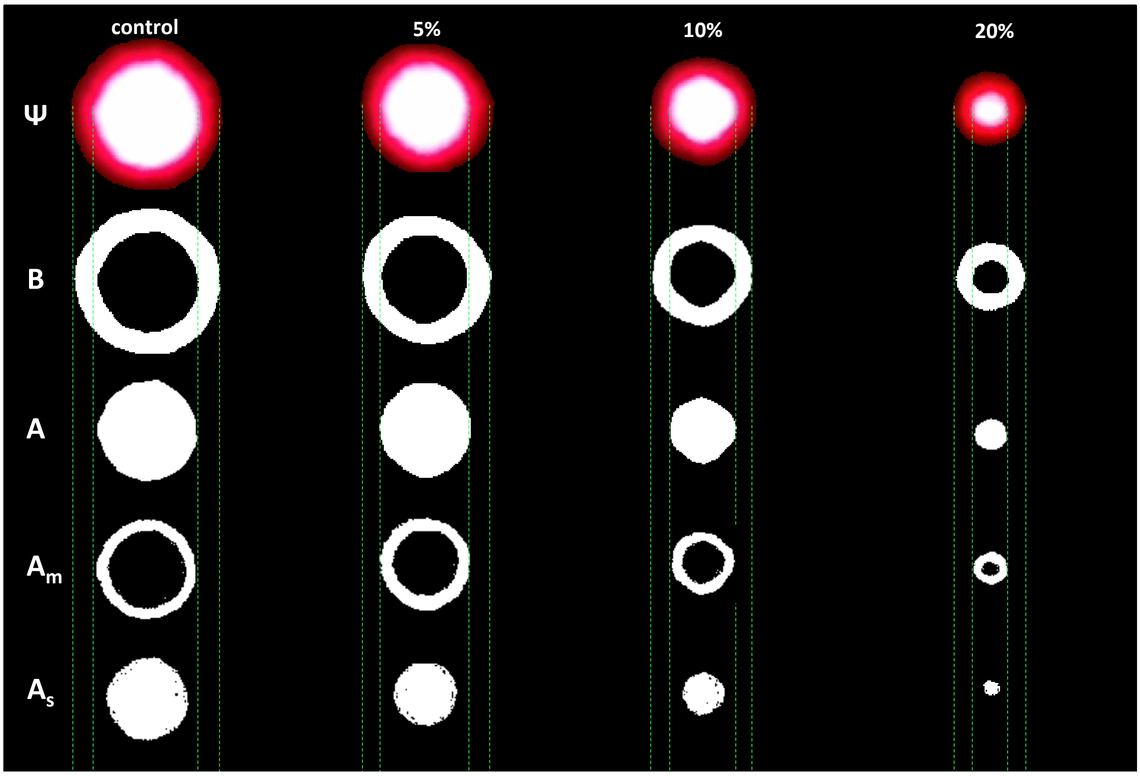

Figure 4. Morphologies of laser backscattering pattern zones from an *AB* sample from each substitution level. Segmented images from Ψ, A, B, A_m and A_s descriptors.

The imaging descriptors data were extracted from all matrix samples both *BB* and *AB*. Figure 4 shows an example of the obtained morphologies for each direct descriptor from an *AB* matrix sample at each substitution level. The observed effect was the reduction of transmitted light (reduction of Ψ) following increasing substitution level. The rest of descriptors followed that behaviour as expected. Thus, the common event was to reduce the absolute value of areas for all direct descriptors but their relationship were not constant.

Figure 5, as an example, shows the behaviour of some indirect descriptors (*A/ Ψ, B/ Ψ, As/ Ψ* and *Am*/ Ψ) data from all *BB* (figure 5 A and B) and AB (figure 5 C and D) samples respectively. It is observed, for both matrixes, how transmittance (*Ψ*), lightest colour zone of *Ψ* (A) and A-saturated (*As*) were reduced with the substitution level. Instead, darkness areas (B) and non-saturated area of *A* (*Am*), which could express the scattered light, increased. On the other hand, the phenomenon presented differences in function of the matrix type. Transmitted light was higher for *BB* samples (30.10^3 pixels) than for AB (10.10^3) although its reduction due to the substitution increases was lower (63% and 85% respectively).

The effect of substitution level was very clear observed in the case of *BB* matrixes, where formulas are presented separately across the obtained curve, excepting 5% and control, which although had not the same values, appeared slightly differenced. This effect was difficulty observed in the case of *AB* matrixes, where although categories were differenced, changes generated in matrix because the heat treatment increase the dispersion along curve and then categories appeared mixed in numerous cases.

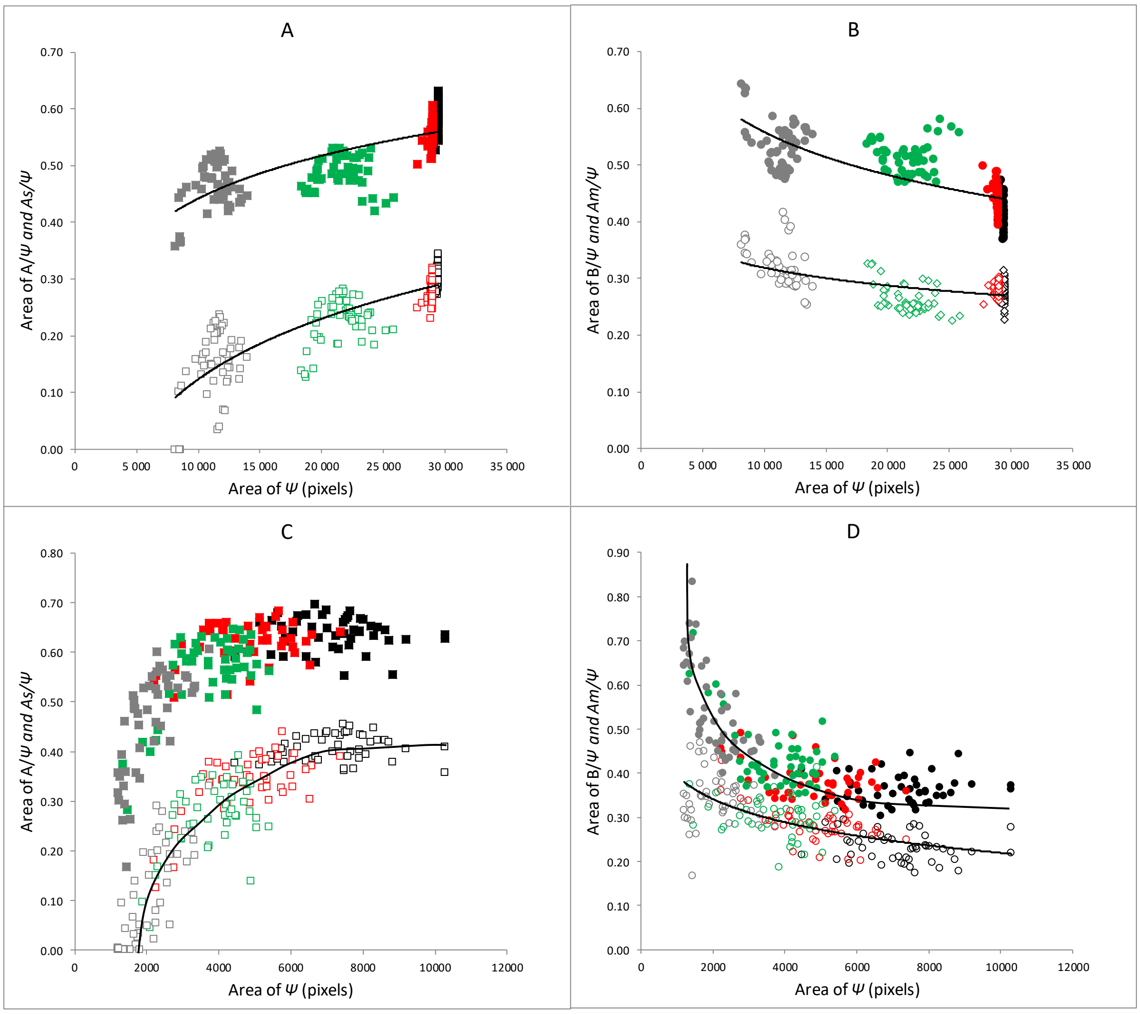

Figure 5. Relation between transmittance (Ψ) and the indirect descriptors: A/Ψ (filled squares), A_s/Ψ (empty squares), B/Ψ (filled circles) and A_m/Ψ (empty circles) for samples control (black), 5% (red), 10% (green) and 20% (grey).

Those differences were produced due to the image descriptors collected variance from only the effect of co-product into the matrix in the case of *BB* matrixes, while in the case of *AB* matrixes the collected variance was the combination of the effect of co-product and heat treatment at time. Thus, the singly effects of both substitution level and heat treatment on the variance collected by image descriptors was evidenced. It meant that the collected information from BB and *AB* was not redundant and then could be combined to improve the characterization of cookies. Based on that, it could be estimated and studied what fraction of the total Ψ variation was generated due to fibre enriching and what by heat treatment on AB matrixes. This approximation was to calculate by the difference between *ΨBB* and *ΨAB*, and then to isolate the part of transmittance reduction produced by changes during baking. The Figure 6 shows the diagram, where the dotted line shows the total variation of Ψ, and the area under the curve is segmented in the two effects above mentioned. There, it can be seen how at 5% enrichment the most variation was produced by the baking, while the change due to the fibre content was increasing following the enrichment. The case of 20% enrichment showed a low weight of baking effect on the total Ψ variation.

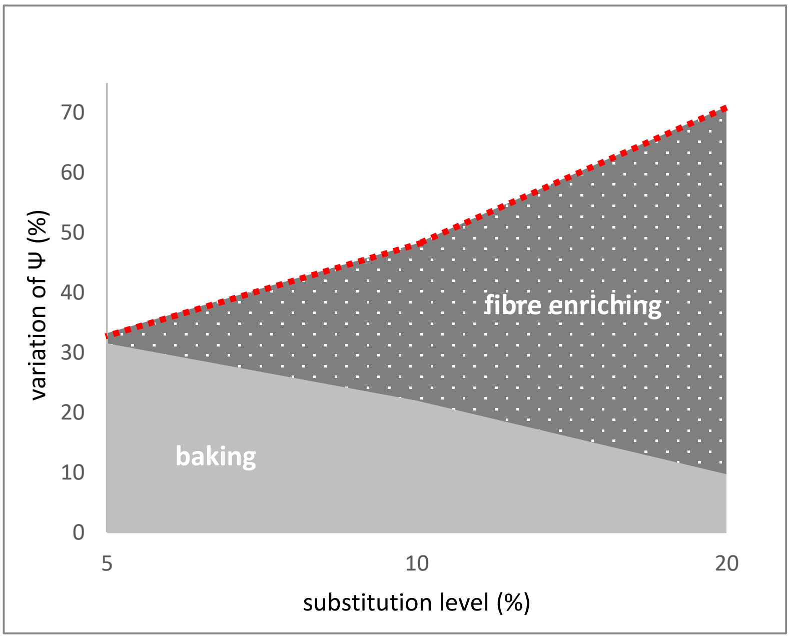

Figure 6. Diagram of *Ψ* total variation charges for fibre enrichment and baking in *AB* matrixes.

---: *Ψ* total variation.

The observed effects are according to previous reported studies where laser backscattering imaging was successful to monitoring modifications on solid food matrices during drying processes, concretely papaya and apple (Romano, Nagle, Argyropoulos, & Müller, 2011; Udomkun, Nagle, Mahayothee, & Müller, 2014). Those experiments show the sensitivity of this technique at modifications in components, water loss and changes of phase from components of those tissues(sugars, proteins, etc.). In this case, fibre enrichment generates the reduction of transmittance by itself because the solid particles of co-product avoid the light trespassing throughout matrix. The fibre enriching also generated cookies with high density (Table 1). This fact explains both the observed reduction of fluxes and the light trespassing because the reduction of matrix porosity.

On the other hand, heat treatment produces a generalized matrix compaction, which explains the higher transmittance of *BB* compared to *AB*. It has implicit phenomena such as an important water loss, protein denaturalization and starch gelatinizations/retrogradation (Barrera, Pérez, Ribotta, & León, 2007). In addition, water loss generates increasing of temperature to develop Maillard and caramelization reactions which modify largely the matrix properties (Purlis & Salvadori, 2009). Thus, these phenomena produce the phase change from viscoelastic to solid matrix, which induce changes on image descriptors. Following the procedure of the study of physicochemical and sensory properties, two PCA based on the 15 descriptors was carried out to determine the characterization capacity of the image descriptors from BB and AB. Figure 3-B and 3-C shows the biplot generated for dough and cookies respectivelly. Both data blocks presented the ordering of samples (points represent the mean value of scores) followed the same order of the physicochemical PCA (Figure 3-A), where samples were situated across PC1, from positive to negative section of this axis, which collected more than 70 % of total variance.

Descriptors were situated in two differenced blocks and positions. The first one was placed within the negative zone of PC1 axis, which collected all indirect descriptors (ratios) related with scatter light indicators all them (B/A_m, B/A_s, A_m/A, A_m/Ψ, B/Ψ and B/A), while the second, placed within positive zone, collected all direct descriptors (Ψ, A, B, A_m, A_s) and the ratios where are implicated saturated zones (A/Ψ and A_s/A). The biplot fitted with behaviour of descriptors evolution analysed in Figure 5. Fibre enriching generates reduction in transmittance and increasing of scatter indicators charge at time. These results allowed confirming that the used descriptors were able to collect the variance produced because fibre enrichment in despite of baking modifications for both type of matrix, which characterized the formulas like using physicochemical and sensory data.

3.3 Modelling studies

After to explore and compare the features of image an physicochemical data, dependence of them was tested by means of regression studies with PLS-R, with the aim of obtaining models for prediction of cookies properties using only image information. Figure 8 shows the results of coefficients for predictions of each single physicochemical and sensory variable and PC1 of physicochemical PCA (Figure 3A) from image data from *BB*, *AB* and both combined. The lowest prediction coefficients were for which obtained from *BB* matrixes data, followed by *AB*, while the predictions done by the combination of both data blocks get the highest ones. That means that information from both matrixes was not redundant. Although information from *AB* was capable to predict better the cookies properties, *BB* matrix information collected high amount of information that complemented the first one, and in addition predict with high coefficient some physicochemical variables by itself.

These differences were according with the above discussed effects of variance charge provided by fibre enrichment and heat treatment separately (Figure 6). The physicochemical behaviour of cookies were governed by both effects, however it seemed that some variables was not dependent of heat modifications, for example the water fluxes (Jw_5 *and* Jw_{10}) and global acceptability (*GA*) having coefficients around than 0.90 with *BB*. Only the effect of fibre enrichment was necessary to know them in this case. On the other hand, the case of the milk was different because it has dissolved, dispersed and emulsified compounds, which had interaction with cookie matrix, generating differences with water, in the same way of the observed differences in Figure 2. These interactions evolved not only by fibre increasing but also by the result of modifications in cookie matrixes because the heat treatment. For that reason, improvement of the predictions for milk fluxes with AB information was according with that fact, which proves the role of the part of total variance collected by *AB* matrixes descriptors related to modifications in matrix during baking. Thus, the complementation of both data blocks (BB+AB) reported prediction coefficients between 0.90-0.97 for all physicochemical parameters excepting *ΔArea*. The incapacity for predicting this parameter could be due the area had not evolution within fibre enrichment levels, only in regard to the control formula. Finally, the prediction of PC1 coordinates was of 0.93, which revealed the possibility of locating any of these formulas into the physicochemical space of variance (physicochemical PCA, Figure 3A) to know its properties by using only the image information.

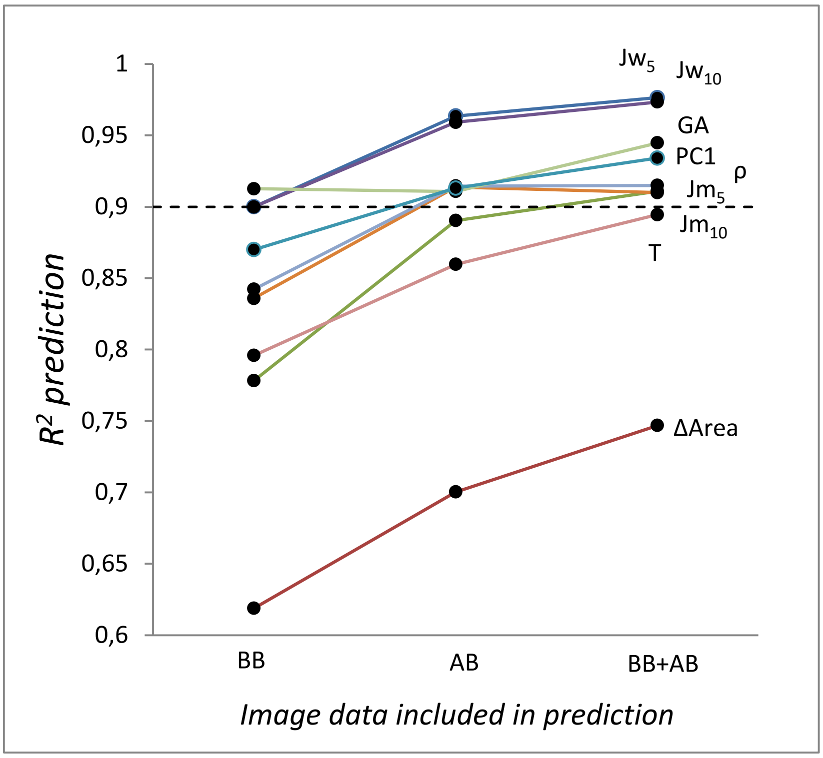

Figure 8. Prediction coefficients (R2) for the physicochemical and sensory properties using image information from matrixes before baking (*BB*), after baking (*AB*) and both combined (*BB+AB*)

4. Conclusions

The results reported that the changes generated by fibre enrichment of cookies produced co-variance on the selected image descriptors, making possible a non-destructive characterization of all cookie formulas. That characterization was got from information of both doughs (matrix before baking) and cookies (matrix after baking). The two matrixes offered complementary information, collecting purely the variance produced by the fibre enrichment in the case of doughs, while in the case of cookies the effect of heat treatment was also registered. When both information blocks were combined, the quantitative prediction of the physicochemical and sensory properties of cookies was improved, both in singly and simultaneously way (PC1). It means that would be better to use both data blocks at time to obtain the best result. Thus, the image analysis of laser scattering patterns by means of the selected descriptors, provided information from which modelling of effect of fibre enrichment on cookies was possible. That means this technique could be used to study cookie properties in a non-destructive mode for both formula developing and on-line quality control of production chain. Based on these results, different configuration of the device has to be tested, as well as others cookie formulas, with the aim of optimizing the laser scattering patterns generation in relationship to cookie properties for collecting the maximum variance. In the same way, new image descriptors could be developed to be applied to other cereal products as crackers, biscuits, toasts, breakfast cereals, etc.

5. Bibliography

Abdul Halim Lim, S., Antony, J., Garza-Reyes, J. A., & Arshed, N. (2015). Towards a conceptual roadmap for Statistical Process Control implementation in the food industry. *Trends in Food Science & Technology*, *44*(1), 117–129. http://doi.org/10.1016/j.tifs.2015.03.002

Adebayo, S. E., Hashim, N., Abdan, K., & Hanafi, M. (2016). Application and potential of backscattering imaging techniques in agricultural and food processing - A review. *Journal of Food Engineering*. http://doi.org/10.1016/j.jfoodeng.2015.08.006

Arendse, E., Fawole, O. A., Magwaza, L. S., & Opara, U. L. (2017). Non-destructive prediction of internal and external quality attributes of fruit with thick rind: A review. *Journal of Food Engineering*. http://doi.org/10.1016/j.jfoodeng.2017.08.009

Barbin, D. F., Kaminishikawahara, C. M., Soares, A. L., Mizubuti, I. Y., Grespan, M., Shimokomaki, M., & Hirooka, E. Y. (2015). Prediction of chicken quality attributes by near infrared spectroscopy. *Food Chemistry*, *168*, 554–60. http://doi.org/10.1016/j.foodchem.2014.07.101

Barrera, G. N., Pérez, G. T., Ribotta, P. D., & León, A. E. (2007). Influence of damaged starch on cookie and bread-making quality. *European Food Research and Technology*, *225*(1), 1–7. http://doi.org/10.1007/s00217-006-0374-1

Chen, Q., Zhang, C., Zhao, J., & Ouyang, Q. (2013). Recent advances in emerging imaging techniques for non-destructive detection of food quality and safety. *TrAC - Trends in Analytical Chemistry*. http://doi.org/10.1016/j.trac.2013.09.007

Fuentes, E., Alcañiz, M., Contat, L., Baldeón, E. O., Barat, J. M., & Grau, R. (2017). Influence of potential pulses amplitude sequence in a voltammetric electronic tongue (VET) applied to assess antioxidant capacity in aliso. *Food Chemistry*, *224*, 233–241. http://doi.org/10.1016/j.foodchem.2016.12.076

Lim, S. A. H., & Antony, J. (2016). Statistical process control readiness in the food industry: Development of a self-assessment tool. *Trends in Food Science & Technology*, *58*, 133–139. http://doi.org/10.1016/j.tifs.2016.10.025

Mireei, S. A., Mohtasebi, S. S., Massudi, R., Rafiee, S., & Arabanian, A. S. (2010). Feasibility of near infrared spectroscopy for analysis of date fruits. *International Agrophysics*, *24*(4), 351–356. Retrieved from https://www.scopus.com/inward/record.uri?eid=2-s2.0-79955023784&partnerID=40&md5=bda54a95925b007416fe8354a2214b79

Mollazade, K., Omid, M., Akhlaghian Tab, F., Kalaj, Y. R., Mohtasebi, S. S., & Zude, M. (2013). Analysis of texture-based features for predicting mechanical properties of horticultural products by laser light backscattering imaging. *Computers and Electronics in Agriculture*, *98*, 34–45. http://doi.org/10.1016/j.compag.2013.07.011

Purlis, E., & Salvadori, V. O. (2009). Modelling the browning of bread during baking. *Food Research International*, *42*(7), 865–870. http://doi.org/10.1016/j.foodres.2009.03.007

Romano, G., Nagle, M., Argyropoulos, D., & Müller, J. (2011). Laser light backscattering to monitor moisture content, soluble solid content and hardness of apple tissue during drying. *Journal of Food Engineering*, *104*(4), 657–662. http://doi.org/10.1016/j.jfoodeng.2011.01.026

Ropodi, a. I., Panagou, E. Z., & Nychas, G.-J. E. (2016). Data mining derived from food analyses using non-invasive/non-destructive analytical techniques; determination of food authenticity, quality & safety in tandem with computer science disciplines. *Trends in Food Science & Technology*, *50*, 11–25. http://doi.org/10.1016/j.tifs.2016.01.011

Sendin, K., Manley, M., & Williams, P. J. (2017). Classification of white maize defects with multispectral imaging. *Food Chemistry*, *243*(September 2017), 311–318. http://doi.org/10.1016/j.foodchem.2017.09.133

Shi, C., Qian, J., Han, S., Fan, B., Yang, X., & Wu, X. (2018). Developing a machine vision system for simultaneous prediction of freshness indicators based on tilapia (Oreochromis niloticus) pupil and gill color during storage at 4 °C. *Food Chemistry*, *243*(May 2017), 134–140. http://doi.org/10.1016/j.foodchem.2017.09.047

Udomkun, P., Nagle, M., Mahayothee, B., & Müller, J. (2014). Laser-based imaging system for non-invasive monitoring of quality changes of papaya during drying. *Food Control*, *42*, 225–233. http://doi.org/10.1016/j.foodcont.2014.02.010

Verdú, S., Barat, J. M., Alava, C., & Grau, R. (2017). Effect of tiger-nut (Cyperus esculentus) milk co-product on the surface and diffusional properties of a wheat-based matrix. *Food Chemistry*, *224*, 69–77. http://doi.org/10.1016/j.foodchem.2016.12.016

Verdú, S., Barat, J. M., & Grau, R. (2019). Non destructive monitoring of the yoghurt fermentation phase by an image analysis of laser-diffraction patterns: Characterization of cow’s, goat’s and sheep’s milk. *Food Chemistry*, *274*(July 2018), 46–54. http://doi.org/10.1016/j.foodchem.2018.08.091

Verdú, S., Vásquez, F., Grau, R., Ivorra, E., Sánchez, A. J., & Barat, J. M. (2016). Detection of adulterations with different grains in wheat products based on the hyperspectral image technique: The specific cases of flour and bread. *Food Control*, *62*, 373–380. http://doi.org/10.1016/j.foodcont.2015.11.002

Wu, Y., Qian, Y., Pan, Y., Li, P., Yang, J., Ye, X., & Xu, G. (2014). Association between dietary fiber intake and risk of coronary heart disease: A meta-analysis. *Clinical Nutrition*. http://doi.org/10.1016/j.clnu.2014.05.009

Xie, C., Chu, B., & He, Y. (2017). Prediction of banana color and firmness using a novel wavelengths selection method of hyperspectral imaging. *Food Chemistry*, *245*(March 2017), 132–140. http://doi.org/10.1016/j.foodchem.2017.10.079

Yang, Y., Zhuang, H., Yoon, S.-C., Wang, W., Jiang, H., & Jia, B. (2018). Rapid classification of intact chicken breast fillets by predicting principal component score of quality traits with visible/near-Infrared spectroscopy. *Food Chemistry*, *244*(17), 184–189. http://doi.org/10.1016/j.foodchem.2017.09.148